

An Analytical Approach to the Spin Distribution of Dark Halos

Tzihong Chiueh

Department of Physics, National Taiwan University, Taipei, Taiwan

chiuehth@phys.ntu.edu.tw

Jounghun Lee

Institute of Astronomy and Astrophysics, Academia Sinica, Taipei, Taiwan

taiji@asiaa.sinica.edu.tw

and

Lihwai Lin

Department of Physics, National Taiwan University, Taipei, Taiwan

d90222005@ms90.ntu.edu.tw

Received _____; accepted _____

ABSTRACT

We derive the distribution of the dimensionless specific angular momentum of dark matter halos, $P(j)$, in the framework of the standard tidal torque theory, and explain the characteristic shape of $P(j)$ commonly observed in N-body simulations. A scalar quantity (shear scalar), r , is introduced for measuring the effective strength of the tidal torque force acting upon the halo from the surrounding matter. It is found that the ubiquitous and broad shape of $P(j)$ can mostly be attributed to the unique property of the shear scalar r , and also that $P(j)$ is insensitive to the underlying collapse dynamics. Our result demonstrates that although the shape of $P(j)$ is ubiquitous and close to log-normal, the distribution is not exactly log-normal but decays exponentially at the high angular momentum end, and drops slowly as a power-law with an index 2 at the low angular momentum end.

Subject headings: cosmology:theory — large-scale structure of universe

1. INTRODUCTION

N-body simulations have shown that the dark matter halos of the universe have the intrinsic angular momentum, the distribution of which has a broad and ubiquitous shape independent of other halo properties such as the halo mass scale, the halo formation epoch, and so on (Barnes & Efstathiou 1987; Heavens & Peacock 1988; Lemson & Kauffmann 1999; Bullock *et al.* 2001; Chen & Jing 2002). This characteristic distribution of the halo angular momentum is often approximated by the log-normal distribution with ubiquitous mean and variance in the log. Although it has been proved that this characteristic distribution can be produced by the current standard model

(Maller *et al.* 2001), the following important questions have yet to be answered: what the physical origin of the characteristic distribution is, and whether it is truly log-normal.

The standard model for the origin and evolution of the halo angular momentum is the tidal torque theory (Doroshkevich 1970; White 1984). In this model, the angular momentum of a proto-halo, \mathbf{L} , is generated by the misalignment of the principal axes of the local shear tensor with that of the inertia tensor and grows with time in the Lagrangian coordinate: $L_i(t) = -a^2(t)\dot{D}(t)\epsilon_{ijk}T_{jl}I_{lk}$. Here, $a(t)$ is the scaling factor, $\dot{D}(t)$ the growing rate of density perturbations, and $I_{lk}(= \int \rho_0 q_l q_k d^3\mathbf{q}$ with ρ_0 being the mean density) is the inertia tensor of a proto-halo site in the Lagrangian \mathbf{q} space, representing the geometrical shape of a proto-halo. In addition, $T_{jl}(= \partial_j \partial_l \phi$ with ϕ being the gravitational potential) is the gravitational shear tensor that quantifies the tidal torque from the surrounding matter.

Strictly speaking, the tidal torque theory is a linear theory, and should break down in the non-linear regime since it does not account for the complicated nonlinear process of halo formation after recollapse. To one’s surprise, however, it has been demonstrated by N-body simulations that the linear tidal torque theory works well even in nonlinear regime (Frenk *et al.* 1988; Heavens & Peacock 1988; Catelan & Theuns 1996; Sugerman *et al.* 2000; Maller *et al.* 2001). Therefore, we will adopt the tidal torque model, and derive the distribution of the halo angular momentum.

2. DERIVATION

2.1. SEPARATION OF THE VARIABLES

For the distribution of halo angular momentum, it is more convenient to use a dimensionless quantity than to use L itself since L scales as $M^{5/3}$: $L \sim I \sim \int q^2 d^3\mathbf{q} \sim R^5 \sim M^{5/3}$, with R and M being the typical size and mass of a proto-halo respectively.

We thus define a time-independent specific angular momentum, j , as $j_i \equiv \epsilon_{ijk} T_{jl} \bar{I}_{lk}$ with $\bar{\mathbf{I}} \equiv \mathbf{I} M^{-5/3}$, since the $\log(j)$ -distribution is evaluated at the same epoch and has a same shape as the $\log(L)$ -distribution, except for a constant horizontal shift.

Rotating the coordinates into the local shear principal axis frame, we find that the magnitude of the specific angular momentum is given as

$$j = \{\bar{I}_{23}^2(\lambda_2 - \lambda_3)^2 + \bar{I}_{31}^2(\lambda_1 - \lambda_3)^2 + \bar{I}_{12}^2(\lambda_1 - \lambda_2)^2\}^{1/2}, \quad (1)$$

where $\lambda_1, \lambda_2, \lambda_3$ are the three eigenvalues of the local shear tensor, and $\bar{I}_{23}, \bar{I}_{31}, \bar{I}_{12}$ are the three off-diagonal components of the dimensionless inertia tensor, $\bar{\mathbf{I}}$. It is worth noting that only the off-diagonal components of the inertia tensor in the shear principal axes are involved in the generation of the halo angular momentum. The diagonal components of the inertia tensor are involved in the gravitational collapse. Interestingly enough, however, it has been recently found by N-body simulations that the shear and inertia tensors are strongly, but not perfectly, aligned (Lee & Pen 2000; Portiani *et al.* 2001b). In other words, in the shear principal axes, the magnitudes of the inertia off-diagonal components are small relative to the diagonal parts. This numerical evidence for the small off-diagonal components of the inertia tensor prompts us to regard the misalignment to be statistical fluctuation and $\bar{I}_{23}, \bar{I}_{31}, \bar{I}_{12}$ as independent random variables. Now that the three eigenvalues of the shear tensor are also random variables, and equation (1) describes how the positive random variable, j , depends on the random variables, $\bar{\mathbf{I}}$ and λ_i 's.

To derive the distribution of j , we first separate the variables as follows. We view the generation of the halo angular momentum as a 3×3 diagonal tidal tensor $R_{ij} \equiv \text{Diag}[r_1, r_2, r_3]$ acting on an inertia-moment vector $\tilde{\mathbf{I}}$, i.e., $j_i = \sqrt{3} R_{ij} \tilde{I}_j$, in the frame of local shear-principal-axis, where the components of R_{ij} and $\tilde{\mathbf{I}}$ are given as $r_1 = (\lambda_2 - \lambda_3)/\sqrt{3}$, $r_2 = (\lambda_3 - \lambda_1)/\sqrt{3}$ and $r_3 = (\lambda_1 - \lambda_2)/\sqrt{3}$, and $\tilde{I}_1 \equiv \bar{I}_{23}$, $\tilde{I}_2 \equiv \bar{I}_{31}$ and $\tilde{I}_3 \equiv \bar{I}_{12}$. As the three components of $\tilde{\mathbf{I}}$ are independent random variables, we may

further express them in spherical-polar coordinates as $\tilde{I}_1 = \tilde{I} \sin \theta \cos \phi$, $\tilde{I}_2 = \tilde{I} \cos \theta$, $\tilde{I}_3 = \tilde{I} \sin \theta \sin \phi$ with $\tilde{I} \equiv (\tilde{I}_1^2 + \tilde{I}_2^2 + \tilde{I}_3^2)^{1/2}$, $\theta \equiv \cos^{-1}(\tilde{I}_2/\tilde{I})$, $\phi \equiv \tan^{-1}(\tilde{I}_3/\tilde{I}_1)$. On the other hand the diagonal components of R_{ij} are not all free but constrained by the condition of $r_1 + r_2 + r_3 = 0$. One may conveniently regard the diagonal components (r_1, r_2, r_3) also as a vector \mathbf{r} ; this vector lies in a plane perpendicular to the $(1, 1, 1)$ symmetric axis in the λ space, or $\mathbf{r} = \lambda \times (1, 1, 1)/\sqrt{3}$. Therefore, \mathbf{r} depends only on one polar angle, say ψ . To find the polar-coordinate expression for \mathbf{r} , we perform a coordinate transformation from $\lambda_1, \lambda_2, \lambda_3$ into x, y, δ , with $x \equiv (\lambda_1 - 2\lambda_2 + \lambda_3)/\sqrt{6}$, $y \equiv (\lambda_1 - \lambda_3)/\sqrt{2}$, $\delta \equiv \lambda_1 + \lambda_2 + \lambda_3$. Under this transformation, \mathbf{r} has only two components: $\mathbf{r} = (x, y, 0)$. So, we can express $x = r \cos \psi$, $y = r \sin \psi$. Now, rotating the axes back into the shear principal axes, we have a polar-angle expression for \mathbf{r} in the shear principal axis frame: $r_1 = -\frac{1}{\sqrt{2}}r \cos \psi + \frac{1}{\sqrt{6}}r \sin \psi$, $r_2 = -\frac{\sqrt{2}}{\sqrt{3}}r \sin \psi$, $r_3 = \frac{1}{\sqrt{2}}r \cos \psi + \frac{1}{\sqrt{6}}r \sin \psi$.

Using these angular variables for $\tilde{\mathbf{I}}$ and \mathbf{r} , we find the following expression for j with separated variables:

$$j = \tilde{I} r Y(\psi, \theta, \phi), \quad (2)$$

where

$$Y(\psi, \theta, \phi) \equiv \left\{ \sin^2 \theta \left(\frac{1}{2} \cos^2 \psi + \frac{1}{6} \sin^2 \psi - \frac{1}{2\sqrt{3}} \cos 2\phi \sin 2\psi \right) + \frac{2}{3} \cos^2 \theta \sin^2 \psi \right\}^{1/2}. \quad (3)$$

The off-diagonal components of the inertia tensor \tilde{I}_1 , \tilde{I}_2 and \tilde{I}_3 are further assumed to be Gaussian variables (Catelan & Theuns 1996). So, the distribution of $\tilde{I} = \sqrt{\tilde{I}_1^2 + \tilde{I}_2^2 + \tilde{I}_3^2}$ is a weighted Gaussian given as $P_{\tilde{I}}(\tilde{I})d\tilde{I} = \sqrt{2/\pi}\sigma_{\tilde{I}}^{-3}\tilde{I}^2 \exp\left(-\tilde{I}^2/2\sigma_{\tilde{I}}^2\right)d\tilde{I}$, where $\sigma_{\tilde{I}}$ is the standard deviation of each off-diagonal component. While the solid angles, ϕ and θ are uniformly distributed on the sphere.

Though the shear scalar r was first pointed out to play an important role for non-spherical halo formation and angular momentum generation by Chiueh & Lee (2001), Sheth & Tormen (2002) recognized that r can in fact be conveniently expressed as $[\frac{2}{15} \sum_{i=1}^5 y_i]^2$

where y_1, \dots, y_5 are mutually independent Gaussian variables, having the same standard deviations equal to that of the density field, σ_δ . Therefore, the distribution of r is also a weighted Gaussian: $P_r(r) = \sqrt{5/\pi}(25/12\sigma_\delta^5)r^4 \exp(-5r^2/4\sigma_\delta^2)$. Sheth & Tormen (2002) commented that the broadness of $P(j)$ may be attributed to the shape of $P_r(r)$. However, $P(j)$ is contributed by the conditional distribution of r only for those regions out of which dark halos condense, i.e., $P_r(r|\text{halo})$, instead of the unconditional $P_r(r)$ given above. In the Press-Schechter model of halo formation (Press & Schechter 1974) where the collapse threshold depends only on δ and not on r , $P_r(r|\text{halo})$ indeed equals $P_r(r)$. However, the actual halo collapse is generically non-spherical, which leads to higher collapse thresholds depending both on δ and r (Sheth *et al.* 2001; Chiueh & Lee 2001). This fact differentiates the actual halo r -distribution per mass bin, $P_r(r|\text{halo})$, from the unconditional $P_r(r)$.

To find $P_r(r|\text{halo})$, we examine the non-spherical collapse using the collapse condition given by Chiueh & Lee (2001): $\frac{\delta}{\delta_c} = \left(1 + \frac{r^4}{\alpha}\right)^\beta$. Chiueh & Lee (2001) originally suggested $\alpha = \beta = 0.15$; later Lin *et al.* (2001) refined the values as $\alpha = 0.26$ and $\beta = 0.16$, which are adopted here. Since the collapse condition depends on r , $P_r(r|\text{halo})$ should no longer equal $P_r(r)$. We calculated $P_r(r|\text{halo})$ numerically using the random-walk method described in Lin *et al.* (2001). Two non-trivial results are found. First, $P_r(r|\text{halo})$ is independent of mass up to the numerical accuracy, and second, $P_r(r)$ turns out to still be a good approximation to $P_r(r|\text{halo})$. Figure 1. compares the numerical $P_r(r|\text{halo})$ near the characteristic mass M_* with $P_r(r)$. The good agreement suggests that the distribution of j is not sensitive to the detailed dynamics of halo formation. This feature is the origin of the scale-independent *shape* of the halo angular momentum distribution to be shown below.

2.2. The j -Distribution

Now, replace $P_r(r|\text{halo})$ by the simpler $P_r(r)$. By equation (2), the angular distribution $P(j)$ can be derived as follows:

$$P(j) = \int d\lambda_1 d\lambda_2 d\lambda_3 \int d\tilde{I} \sin \theta d\theta d\phi P_\lambda(\lambda_1, \lambda_2, \lambda_3) P_{\tilde{I}} \delta_D(j - \tilde{I} r Y(\theta, \phi, \psi)), \quad (4)$$

where

$$P_\lambda(\lambda_1, \lambda_2, \lambda_3) = \frac{3375}{8\sqrt{5}\pi\sigma_\delta^6} \exp\left(-\frac{\delta^2}{2\sigma_\delta^2} - \frac{5r^2}{4\sigma_\delta^2}\right) |(\lambda_1 - \lambda_2)(\lambda_2 - \lambda_3)(\lambda_1 - \lambda_3)|, \quad (5)$$

and the Dirac δ_D -function constrains j to other variables through eq.(2). Note that the last factor in eq.(5) is no more than $|r_1 r_2 r_3| (\equiv J(r, \psi))$, arising from the Jacobian of the angular distribution of the shear principal axes (Doroshkevich 1970). Thus, $J(r, \psi) = r^3 J(\psi)$, with $J(\psi) \equiv |(3 \cos^2 \psi - \sin^2 \psi) \sin \psi|$. The angular dependence of $J(\psi)$ results in P_λ to contain three null lines, separated by 60 degrees, on the plane where the \mathbf{r} vector lies. The null lines correspond to the degeneracies, $\lambda_1 = \lambda_2$, $\lambda_2 = \lambda_3$ and $\lambda_3 = \lambda_1$. This feature renders the random angle ψ to distribute non-uniformly with three-fold symmetry.

Upon changing the variables from $\lambda_1, \lambda_2, \lambda_3$ to δ, r, ψ , the δ, \tilde{I} and r integrals can all be evaluated analytically, and eq.(4) now becomes

$$P(j) = w^{-1} j^3 \int \frac{d^3 \Omega}{Y^4} K_1\left(\sqrt{\frac{5}{2}} \frac{j}{bY}\right) J(\psi) \quad (6)$$

where $d^3 \Omega \equiv \sin \theta d\theta d\phi d\psi$, K_1 is the 1st-order modified Bessel function, $b \equiv \sqrt{\sigma_\delta \sigma_{\tilde{I}}}$, w the normalization factor and Y is given in eq.(3). As $\log(j/b) = \log(j) - \log(b)$, the shape of the $\log(j)$ -distribution is not affected by the value of the unknown b although the peak position is. The angular integration of eq.(6) can only be evaluated numerically and the solid line of Figure 2 presents the resulting $jP(j)$. It shows that though the main body of $P(j)$ resembles the log-normal distribution (dashed line), the distribution is not exactly log-normal. One may check from eq.(6) by asymptotic expansion that $P(j)$ drops off

exponentially at the high angular momentum limit (cf. Maller *et al.* 2001) and behaves as a power law ($\sim j^2$) in the lower angular momentum limit. The best-fit log-normal to our distribution has a log-width $\sigma_{\log j} = 0.63$ (dashed line), which is in fair agreement with the log-width, $\sigma_{\log j} = 0.5$, obtained from N-body simulations reported by Bullock *et al.* (Bullock *et al.* 2001). (Their definition of λ' is equivalent to our j modulo a constant factor.)

For comparison, we have also simulated non-spherical halo collapse using the random-walk algorithm. When the collapse condition given in the previous section is satisfied, the shear tensor is diagonalized (Chiueh and Lee, 2001) and the three principal eigenvalues λ' s are used to evaluate the halo shear vector \mathbf{r} . The angular momentum of the dark halo is then computed according to eq.(1). Figure 2 also plots the resulting $jP(j)$ (solid squares). To ensure the accuracy of the our method, we have also repeated the same procedure for the Press-Schechter model and computed its $jP(j)$ (solid triangles), to which the solid line should be identical. As one can see, all three results agree with each other, revealing that the angular momentum distribution is insensitive to the detailed dynamics of halo formation.

We would like to stress that the unique shape and $\log(j)$ width of the angular-momentum distribution are the direct outcome of our model. It involves no fitting parameter.

3. DISCUSSIONS AND CONCLUSIONS

To explain the observed characteristic shape for the angular momentum distribution of dark halos in N-body simulations, we have adopted the standard tidal torque theory to study the proto-halo angular momentum j_i , which can succinctly be represented by a random

shear R_{ij} acting upon a random vector \tilde{I}_i . The diagonalized R_{ij} , whose three components are the mutual differences of the three eigenvalues of the local shear tensor, quantifies the non-sphericity of the local gravitational potential, and the vector $\tilde{\mathbf{I}}$ characterizes the misalignment between the matter distribution and local gravitational potential. With this picture, we have derived a new expression for the halo angular momentum, which separates the variables into three parts: $r, \tilde{I}, Y(\psi, \theta, \phi)$. With $P_r(r|\text{halo})$ being shown to be approximately a weighted Gaussian and assuming $P_{\tilde{I}}(\tilde{I})$ to also be a weighted Gaussian, we have derived the angular-momentum distribution, i.e., $P(j)$, to be close to log-normal, with a mass-independent width in fair agreement with that determined from simulations. This "quasi"-log-normal distribution is simply a consequence of the nonlinear coupling of five random variables, $r, \tilde{I}, \theta, \phi$ and ψ .

Though the distribution of $\log(j)$ has a mass-independent shape, the mean of $\log(j)$ is predicted to depend on b ($\equiv \sigma_{\tilde{I}}\sigma_{\delta}(M)$). As our framework does not permit the mass dependence of $\sigma_{\tilde{I}}$ to be determined, this present work can only account for the ubiquitous *shape*, but not the peak location, of the angular momentum distribution. Nonetheless, simulations have empirically found that even the mean value of $\log j$ is also mass independent (Barnes & Efstathiou 1987; Heavens & Peacock 1988; Lemson & Kauffmann 1999; Bullock *et al.* 2001; Chen & Jing 2002). Incorporating this finding, we thus demand that

$$\sigma_{\tilde{I}}(M) \propto \sigma_{\delta}^{-1}(M). \quad (7)$$

Such mass dependence of $\sigma_{\tilde{I}}$ is turned to be the prediction of the present work. That is, the misalignment (per mass) \tilde{I} has a wider distribution for larger halos than for smaller halos at the same epoch, since σ_{δ} is greater for smaller halos than for larger halos. This prediction does make qualitative sense, in that at a given epoch large halos have undergone vigorous growth with mergers of sub-halos; it thus makes the interior matter distribution of large halos less correlated with the surrounding matter from which the gravitational forces are

exerted. By contrast, small halos have grown mildly and hence tend to be in a quiescent state, thus keeping themselves well correlated with the surrounding matter. At any rate, this prediction as well as the Gaussianity assumption of \tilde{I} are both testable by cosmological simulations.

This work has been supported by the Taida-ASIAA CosPA Project. T.C. acknowledges the partial support from the National Science Council of Taiwan under the grant: NSC90-2112-M-002-026.

REFERENCES

- Barnes, J., & Efstathiou, G. 1987, *ApJ*, 39, 575
- Bullock, J. S., Dekel, A., Kolatt, T. S., Kravtsov, A. V., Klypin, A. A., Porciani, C., & Primack, J. R. 2001, *ApJ*, 55, 240
- Catelan, P., & Theuns, T. 1996, *MNRAS*, 282, 436
- Chen, D. N., & Jing, Y. P. 2002, preprint (astro-ph/0201520)
- Chiueh, T., & Lee, J. 2001, *ApJ*, 555, 83
- Doroshkevich, A. G. 1970, *Astrofisika*, 6, 581
- Frenk, C. S., White, S. D. M., Davis, M., & Efstathiou, G., 1988, *ApJ*, 327, 507
- Heavens, A. F., & Peacock, J. A. 1988, *MNRAS*, 232, 339
- Lee, J., & Pen, U. 2000, *ApJ*, 532, L5
- Lemson, G., & Kauffmann, G. 1999, *MNRAS*, 302, 111
- Lin, L., Chiueh, T., & Lee, J. 2001, to appear in *ApJ*(astro-ph/0112380)
- Maller, A. H., Dekel, A., & Somerville, R. S. 2001, preprint (astro-ph/0105168) Portiani, C.
Dekel, A., & Hoffman, Y. 2001, preprint (astro-ph/0105123)
- Portiani, C. Dekel, A., & Hoffman, Y. 2001, preprint
- Press, W. H., & Schechter, P. 1974, *ApJ*, 187, 425
- Sheth, R., & Tormen, G. 2002, *MNRAS*, 329, 61
- Sheth, R. K., Mo, H. J., & Tormen, G. 2001, *MNRAS*, 323, 1

Sugerman, B., Summers, F. J., & Kamionkowski, M. 2000, MNRAS, 311, 762

Vitvitska, M, Klypin, A. A., kravtsov, A. V., Bullock J. S., Wechsler, R. H., & Primack, J.
R. 2001, preprint (astro-ph/005349)

White, S. D. M. 1984, ApJ, 286, 38

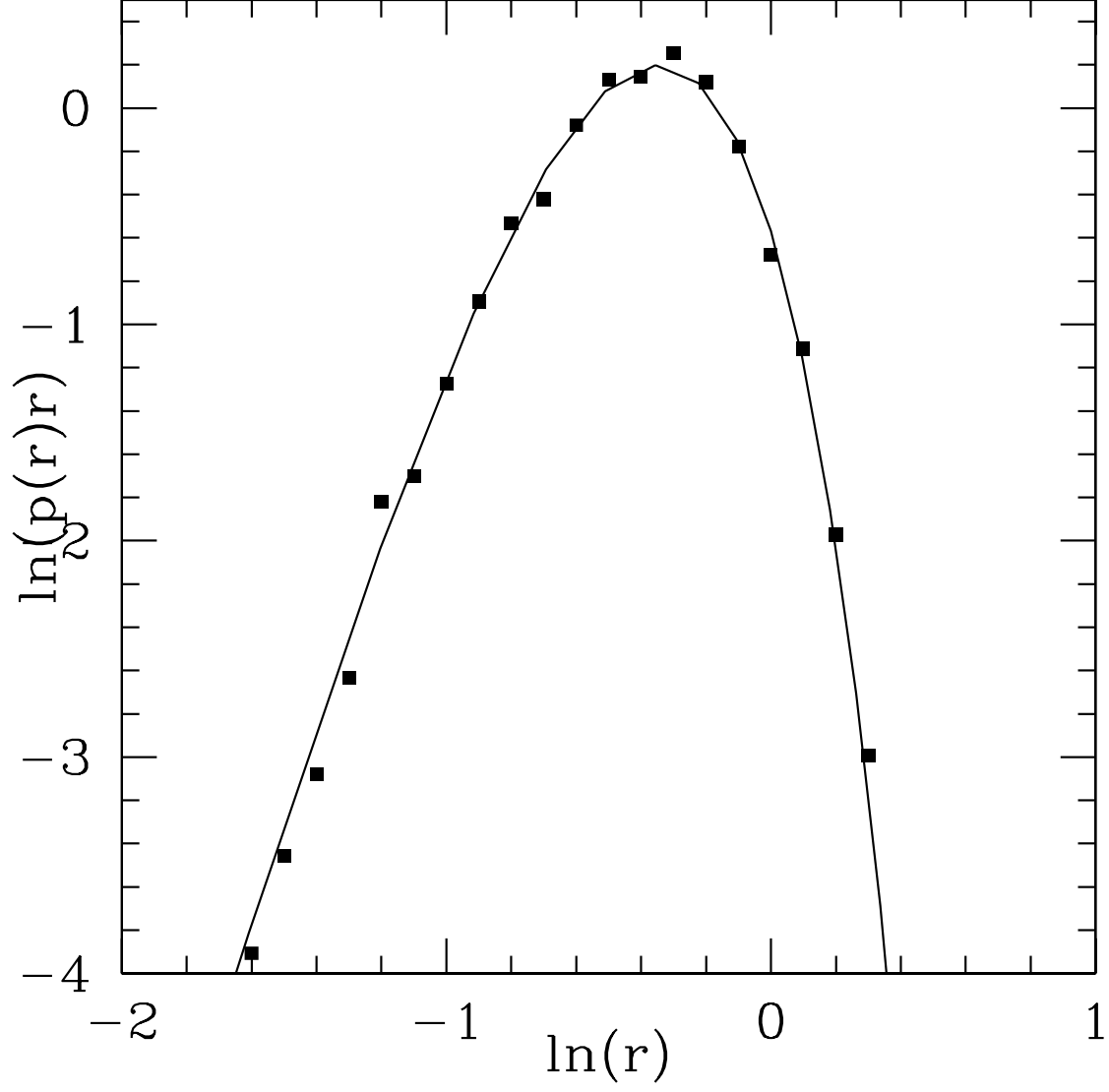


Fig. 1.— The distribution of the halo shear scalar r in the logarithmic scale. The solid squares are $P_r(r|\text{halo})$ near M_* obtained from the Monte-Carlo simulation using the non-spherical collapse condition. The solid curve is $P_r(r)$ given by the analytic formula with the Press-Schechter collapse condition.

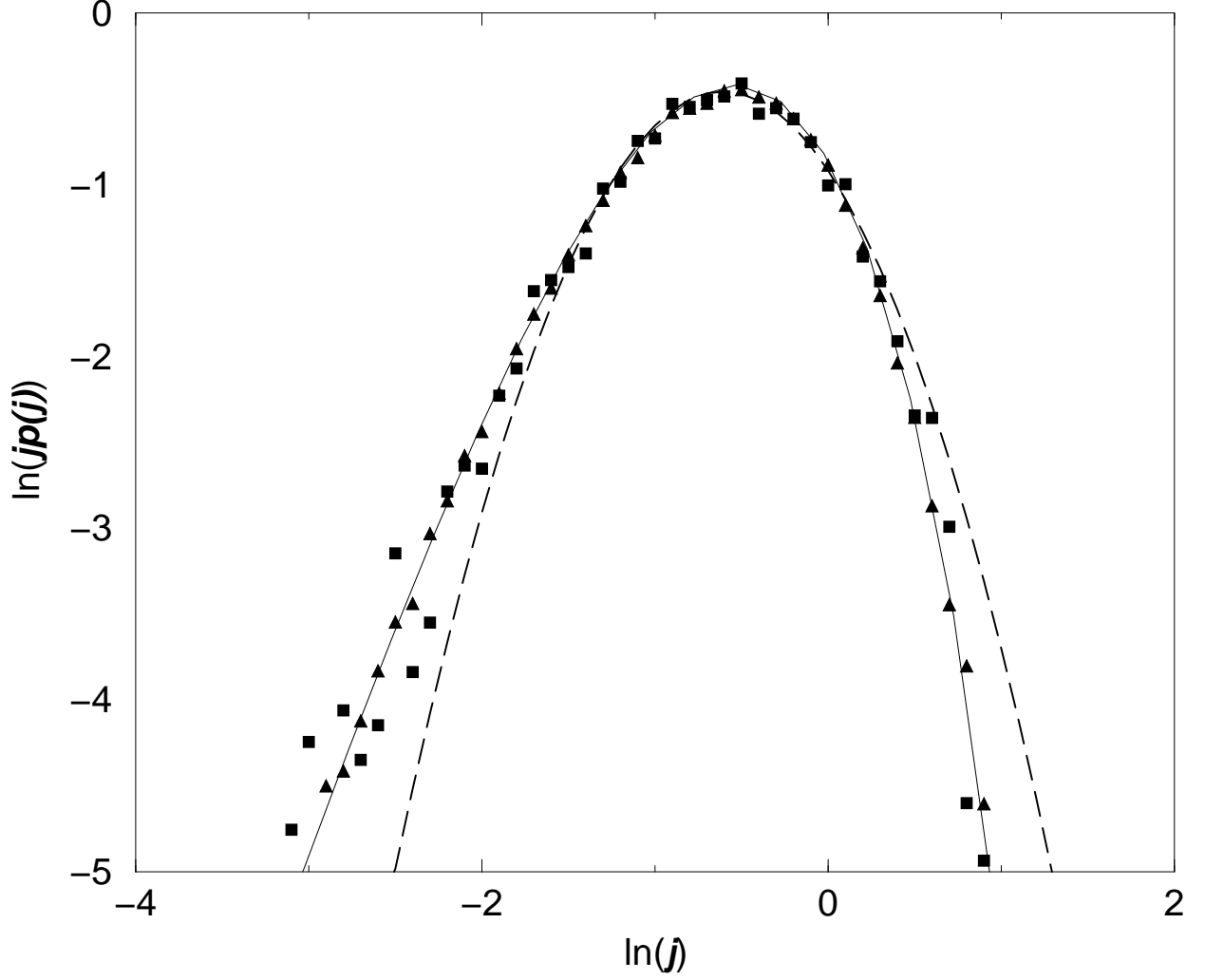


Fig. 2.— The distribution of the logarithmic specific angular momentum of dark halos, $jP(j)$. The solid curve is our analytic result given by eq.(6); the squares are Monte Carlo result for the non-spherical dynamical model, and the triangles are Monte Carlo result for the Press-Schechter model. The dashed line is the best log-normal fit to $jP(j)$.